Standard Title Page - Report on State Project

Report No.	Report Date	No. Pages	Type Report: Final	Project No.: 70983
VTRC 05-CR9	January 2005	36	Period Covered: 10/01/03 to 12/31/04	Contract No. 04-0627-10

Title:
Field Investigation of High Performance Pavements in Virginia

Key Words: Pavement design, field evaluation, GPR, FWD, Smoothens, Resilient Modulus, Creep Compliance.

Authors:

Gerardo W. Flintsch, Ph.D., P.E., Imad L. Al-Qadi, Ph.D., P.E., Amara Loulizi, Ph.D., P.E., Samer Lahouar, Ph.D., Kevin McGhee, P.E., and Trenton Clark, P.E.

Performing Organization Name and Address:

Virginia Tech Transportation institute
3500 Transportation Research Plaza
Blacksburg, VA 22903

Sponsoring Agencies' Name and Address

Virginia Department of Transportation
1401 E. Broad Street
Richmond, VA 23219

Supplementary Notes

Supplemental appendices containing the field data collected for this investigation are available upon request.

Abstract

This study evaluated 18 pavement sections located in high-traffic highways in Virginia to find a premium pavement design with a life span of 40 years or more using current and past field experience. The selected pavement sections were thought to perform well. Eight flexible pavements, six composite pavements, two continuously reinforced concrete pavements, and two jointed plain concrete pavements were investigated. Field testing consisted of (1) falling weight deflectometer (FWD) testing to assess the structural capacity of the different pavements and to backcalculate the pavement layer materials' moduli, (2) ground-penetrating radar (GPR) scanning to determine layer thicknesses and to locate any abnormalities inside the pavements, (3) digital imaging to determine condition indices, (4) longitudinal profile measurements to calculate International Roughness Index, and (5) coring and boring to perform material characterization of pavement layers. Hot mix asphalt tests included resilient modulus and creep compliance. Concrete was tested for compressive strength.

The analysis of the collected data suggests that premium pavement designs can be obtained. The field investigations suggest that all the tested sites are performing satisfactorily and show very low structural distress. Limited material-related problems were found at some sites, which induced non-load related distresses. It was also confirmed that FWD, GPR, and digital imaging are very useful tools to assess the condition of existing pavements.

Since the three categories of pavements (flexible, composite, and rigid) were found to perform well, the study recommends that evaluation of other pavement sections, which are thought to perform in a less than optimal state, be conducted to define the causes of the less than desired performance.

The selection of the most appropriate premium pavement design should be based on a detailed life-cycle cost analysis; hence, such analysis should be performed. Mechanistic empirical modeling of the best performing section within each category would allow the prediction of future pavement performance for use in the life-cycle cost analysis.

Copyright by the Virginia Center for Transportation Innovation and Research. Gerardo W. Flintsch, Ph.D., P.E., Imad L. Al-Qadi, Ph.D., P.E., Amara Loulizi, Ph.D., P.E., Samer Lahouar, Ph.D., Kevin McGhee, P.E., and Trenton Clark, P.E. "Field Investigation of High Performance Pavements in Virginia," Virginia Transportation Research Council 530 Edgemont Road Charlottesville, VA 22903, Report No. VTRC 05-CR9, Jan. 2005.

FINAL CONTRACT REPORT

FIELD INVESTIGATION OF HIGH PERFORMANCE PAVEMENTS IN VIRGINIA

Gerardo W. Flintsch, Ph.D., P.E.
Roadway Infrastructure Group Leader, VTTI, Virginia Tech

Imad L. Al-Qadi, Ph.D., P.E.
Founder's Professor of CEE, University of Illinois at Urbana-Champaign

Amara Loulizi, Ph.D., P.E.
Research Scientist, VTTI, Virginia Tech

Samer Lahouar, Ph.D.
Senior Research Associate, VTTI, Virginia Tech

Kevin K. McGhee, P.E., Senior Research Scientist
Virginia Transportation Research Council

Trenton Clark, P.E., Asphalt Pavement Field Engineer
Virginia Department of Transportation, Materials Division

Project Manager
Kevin K. McGhee, P.E., Virginia Transportation Research Council

Contract Research Sponsored by
Virginia Transportation Research Council

Virginia Transportation Research Council
(A Cooperative Organization Sponsored Jointly by the
Virginia Department of Transportation and
the University of Virginia)

Charlottesville, Virginia

February 2005
VTRC 05-CR9

NOTICE

The project that is the subject of this report was done under contract for the Virginia Department of Transportation, Virginia Transportation Research Council. The contents of this report reflect the views of the authors, who are responsible for the facts and the accuracy of the data presented herein. The contents do not necessarily reflect the official views or policies of the Virginia Department of Transportation, the Commonwealth Transportation Board, or the Federal Highway Administration. This report does not constitute a standard, specification, or regulation.

Each contract report is peer reviewed and accepted for publication by Research Council staff with expertise in related technical areas. Final editing and proofreading of the report are performed by the contractor.

Copyright 2005 by the Commonwealth of Virginia.

ABSTRACT

This study evaluated 18 pavement sections located in high-traffic highways in Virginia to find a premium pavement design with a life span of 40 years or more using current and past field experience. The selected pavement sections were thought to perform well. Eight flexible pavements, six composite pavements, two continuously reinforced concrete pavements, and two jointed plain concrete pavements were investigated. Field testing consisted of (1) falling weight deflectometer (FWD) testing to assess the structural capacity of the different pavements and to backcalculate the pavement layer materials' moduli, (2) ground-penetrating radar (GPR) scanning to determine layer thicknesses and to locate any abnormalities inside the pavements, (3) digital imaging to determine condition indices, (4) longitudinal profile measurements to calculate International Roughness Index, and (5) coring and boring to perform material characterization of pavement layers. Hot mix asphalt tests included resilient modulus and creep compliance. Concrete was tested for compressive strength.

The analysis of the collected data suggests that premium pavement designs can be obtained. The field investigations suggest that all the tested sites are performing satisfactorily and show very low structural distress. Limited material-related problems were found at some sites, which induced non-load related distresses. It was also confirmed that FWD, GPR, and digital imaging are very useful tools to assess the condition of existing pavements.

Since the three categories of pavements (flexible, composite, and rigid) were found to perform well, the study recommends that evaluation of other pavement sections, which are thought to perform in a less than optimal state, be conducted to define the causes of the less than desired performance.

The selection of the most appropriate premium pavement design should be based on a detailed life-cycle cost analysis; hence, such analysis should be performed. Mechanistic empirical modeling of the best performing section within each category would allow the prediction of future pavement performance for use in the life-cycle cost analysis.

FINAL CONTRACT REPORT

FIELD INVESTIGATION OF HIGH PERFORMANCE PAVEMENTS IN VIRGINIA

Gerardo W. Flintsch, Ph.D., P.E.
Roadway Infrastructure Group Leader, VTTI, Virginia Tech

Imad L. Al-Qadi, Ph.D., P.E.
Founder's Professor of CEE, University of Illinois at Urbana-Champaign

Amara Loulizi, Ph.D., P.E.
Research Scientist, VTTI, Virginia Tech

Samer Lahouar, Ph.D.
Senior Research Associate, VTTI, Virginia Tech

Kevin K. McGhee, P.E., Senior Research Scientist
Virginia Transportation Research Council

Trenton Clark, P.E., Asphalt Pavement Field Engineer
Virginia Department of Transportation, Materials Division

INTRODUCTION

The American Association of State Highway and Transportation Officials (AASHTO) is currently moving toward a mechanistic empirical design methodology for pavement design. This approach will consider material properties, truck traffic volumes, loads and spectra, tire pressures, and other parameters not incorporated in traditional design practices. This new approach may take several years to be validated and implemented in Virginia. Unfortunately, some sections of high priority corridors such as I-64 and I-81 require major rehabilitation and reconstruction in the next few years and cannot wait for new design processes to be validated and implemented. The current AASHTO approach, complemented with extensive field experience, may be used after appropriate modification and verification using advanced analytical schemes that account for uncertainties in traffic volume and loading characteristics.

PURPOSE AND SCOPE

The ultimate objective of this project was to develop a premium pavement design with a life span of 40 years or more, using advanced modeling along with current and past field experience. The program was initially planned in two phases. This report documents the results of Phase I of the project, in which the research team performed field evaluations and analysis of existing pavements. The team also conducted laboratory testing and analysis of the hot-mix asphalt (HMA) and concrete layers of selected test pavement sections.

METHODS AND MATERIALS

The first task of this project was to perform an in-depth field evaluation and analysis of in-service pavements from designated high-priority routes. In total, 18 pavement sections were evaluated. Table 1 presents a summary of the selected test sections. The sections were located primarily on interstate highways and other high-traffic routes. The field evaluation included the use of ground-penetrating radar (GPR) for determining pavement layer thicknesses, a falling-weight deflectometer (FWD) for determining the moduli of the pavement layers, visual and video surveys of the pavement surfaces for determining distress types and quantities, and friction and smoothness measurement to determine the functional condition of the test sections.

To avoid excessive delays to the public during field evaluation, the section lengths were set at 0.8 km (0.5 mi). It should be noted that this length also helped achieve uniformity of the pavement structure along the tested section. Since the selected test sites were high-priority and heavily traffic routes, testing was carried out at off-peak hours, usually at night. Traffic control established complete lane closure for the entire 0.8 km (0.5 mi) of each test section plus an additional 0.16 km (0.1 mi) at the beginning and end. A limited number of cores were taken from each site. In addition to measuring the thickness in order to check GPR predicted values, the cores were tested in the lab to measure their engineering properties. Detailed information about each site and the test conducted is available from the authors.

Table 1. Selected high performance pavement test sites

Site #	County	Route	Direction	Milepost*	Pavement Type^	Pavement Age/Surface Age (yrs)
01	Amherst	US-29	South	7.80-7.30	Flexible	34 / 11
02	Albemarle	I-64	East	12.99-13.37	Comp. CRCP (rehab)	34 / 12
03	Louisa	I-64	West	9.91-9.41	Flexible	34 / 9
04	Louisa	I-64	West	2.28-1.78	CRCP	17 / 17
05	New Kent	I-64	East	14.69-15.19	Comp. CRCP (rehab)	32 / 13
06	York	I-64	West	2.62-2.12	Flexible	25 / 7
07	York	I-64	West	22.23-24.71	JPCP	7 / 7
08	Suffolk	US-58	East	25.50-26.00	Comp. JRCP (rehab)	72 / 1
09	Henrico	I-295	South	5.29-5.79	Comp. CRCP (rehab)	23 / 6
10	Hanover	I-295	South	9.52-10.02	Comp. CRCP (rehab)	24 / 9
11	Prince George	I-295	South	8.37-8.87	CRCP	12 / 12
12	Greensville	I-295	North	5.50-6.00	Comp. JPCP (rehab)	14 / 6
13	Fairfax	I-66	West	8.20-7.82	JPCP	8 / 8
14	Russell	I-19	North	8.68-9.18	Flexible	6 / 6
15	Rockbridge	I-81	South	22.92-22.42	Flexible	37 / 17
16	Frederick	I-81	North	21.31-21.87	Flexible	39 / 13
17	Washington	I-81	South	12.50-12,00	Flexible	42 / 11
18	Washington	I-81	South	1.50-1.00	Flexible	5 / 3

* County Milepost

^ CRCP = Continuously Reinforced Concrete Pavement
JPCP = Jointed Plain Concrete Pavement

GPR Testing

Ground-penetrating radar was used in this project to determine layer thickness of the selected pavement sections and to detect any localized subsurface distresses within the layers. The GPR system used was a SIR-10B control unit, manufactured by Geophysical Survey Systems, Inc. (GSSI), connected to a 1-GHz air-coupled antenna and a 1.5-GHz ground-coupled antenna.

All GPR surveys were conducted using the test van depicted in Figure 1. The van has an antenna fixture in the back that permits deployment of the GPR antennas at three transverse locations (right wheel path, center, and left wheel path). Additionally, the van has a high resolution distance measuring instrument (DMI) connected to its back wheel that allows accurate triggering of GPR scans at user-fixed intervals.

Figure 1. Van used for GPR data collection

With the exception of Site 18, GPR surveys were conducted in the travel lane of each site at two transverse locations: the center of the lane; and the right wheel path. For Site 18, the third lane contained the pavement test section; therefore the GPR testing was in the center and the left wheel path. Depending on the surveyed pavement structure, the air-coupled antenna was used alone or simultaneously with the ground-coupled antenna to collect the GPR data at fixed intervals, starting from the beginning of the sites. The choices of the antennas and the GPR acquisition rate were based on the following criteria:

1. For the flexible sections, GPR data were collected using the air-coupled antenna at an acquisition rate of one scan per 0.3 m (1 ft). In this case, the test was performed at speeds ranging between 48 and 65 km/h (30 and 40 mph).
2. For the jointed plain concrete and composite sections (HMA over jointed plain concrete), GPR data were collected simultaneously by the air-coupled and ground-coupled antennas. Because of its deep penetration, the data collected by the ground-coupled antenna was used to get qualitative information (such as prominent distress

locations) about the deep layers, whereas the air-coupled antenna data were used to estimate the layer's thickness. For these sections, data were collected at a rate of one scan per 0.3 m (1 ft). The test speed was limited in this case by the ground-coupled antenna to 8 km/h (5 mph).

3. For the composite sections incorporating reinforcement, GPR data were collected simultaneously by the air-coupled and ground-coupled antennas. In order to detect the transverse reinforcement reflections in the GPR data, the data acquisition rate was set in this case at one scan per 25 mm (1 in). The test speed was limited in this case by the ground-coupled antenna to 8 km/h (5 mph).

Even though the data acquisition was controlled during all of the GPR runs by the DMI, the beginning and the end of each site were also marked using a manual push-button marker, which placed a clear mark in the data. These marks were used during the data analysis to identify the exact limits of the sites.

Furthermore, stationary GPR measurements (i.e., collected while the GPR van was stopped) were taken near the core locations prior to coring and boring. These measurements were used to validate the GPR thickness results and to estimate their accuracy.

FWD Testing

FWD measurements were performed to determine the current structural capacity of each test site under evaluation. The deflections measured by the FWD were utilized to estimate the *in situ* moduli of the various layers of the tested pavement systems using backcalculation software packages.

All tests were conducted using the Virginia Department of Transportation (VDOT) Dynatest model 8002 FWD unit. The three main components of this system include: (1) Dynatest 8002-054 FWD Trailer, (2) Dynatest 9000 system processor, and (3) Gateway laptop computer. The peak deflections caused by the applied load are registered by nine sensing transducers (geophones). Sensors located at 0, 203, 305, 457, 610, 914, 1219, 1524 and 1829 mm (0, 8, 12, 18, 24, 36, 48, 60 and 72 in) from the center of the loading plate were used in all sites. Fourteen drops were applied at each FWD testing point including two seating drops of 40 kN (9,000 lb), and three drops at each of the following load levels: 26.7 kN (6,000 lb), 40 kN (9,000 lb), 53.4 kN (12,000 lb), and 71.2 kN (16,000 lb).

Three types of tests were performed: (1) standard basin tests (for flexible, composite, CRCP, and JPCP pavements); (2) load transfer across cracks (for CRCP); and (3) load transfer across joints (for JPCP). Load transfer across cracks or joints was performed to evaluate the load transfer efficiency using the same sensor spacing and load levels as the standard basin tests. The crack or joint was left between the loading plate and Sensor 3 (305 mm from loading plate). The location of Sensor 2 (203 mm from loading plate) varies from test to test.

The test frequency and location varied for each pavement type, but in general, the following frequencies were used:

1. Flexible Pavement:
    - Basin test: every 15.24 m (50 ft) on the right wheel path.
2. Composite Pavement:
    - Basin test: every 15.24 m (50 ft) on the center of the lane (between wheel paths).
3. Continuously Reinforced Concrete Pavement:
    - Basin test: every 30.48 m (100 ft) on the center of the lane.
    - Load Transfer across cracks: one crack every approximately 30.48 m (100 ft).
4. Jointed Plain Concrete Pavement:
    - Basin test: every 45.72 m ± 6.10 m (150 ft ± 20 ft) on the slab's center.
    - Load transfer across joints: every 15.24 m ± 3.05 m (50 ft ± 10 ft) on the right wheel path.

Two sets of temperature data were collected during FWD testing: pavement surface temperature (using a Raytek temperature sensor); and air temperature (using the Dynatest temperature sensor).

Visual/Video Survey

A visual survey of the pavement surface condition was performed to determine the degree of structural and functional distress present in the pavement. The distress was obtained from video of the surface taken by a high-speed, downward-facing digital video camera.

Figure 2. Deployment of the digital camera used for the video survey

As depicted in Figure 2, the digital camera used to collect the video was fixed to the GPR van and was synchronized with the same DMI used to control the GPR data acquisition. The digital camera provided 24-bit color images of the surface with a resolution of 656×494 pixels. To get clear images of the surface even during high-speed surveys, the camera has a high shutter speed (exposure time as low as 20 ms) and a high frame rate (up to 75 frames/s).

For the sites that were tested during the day, two digital videos were collected concurrently with the GPR measurements, which were centered on the right wheel path and the lane center. Because the van is not equipped with lights that can be used to collect video at night, all sites that were tested with the GPR at night were filmed the next day. No lane closure was required in the latter case because the videos were taken at speeds above 72 km/h (45 mph).

At the selected height and using wide-angle lenses, the video camera captured 4.3 m × 3.6 m (14 ft × 12 ft) frames that covered the whole lane. Based on this frame size, the surface images were collected for most sites at 3 m (10 ft) with spacing starting from the beginning of the test sections. However, for some sites, in which part of the video was obscured by the shadow of the van, the images were taken at 1.5 m (5 ft) spacing. The image overlap allowed removal of the shadow effects during the analysis.

Coring/Boring

Coring and boring were conducted in all of the sections to verify pavement layer thickness, evaluate the *in situ* condition of the materials and to extract samples for material characterization in the laboratory. Samples of pavement materials were obtained at predetermined locations.

When sampling HMA materials, 150 mm (6-in) cores were taken through the layer. The 150 mm (6-in) size was necessary for anticipated testing of the larger stone base mixtures. Ten cores were extracted from each full-depth HMA section. The cores were extracted every 60 m (200 ft) along the test sections, alternating between the right wheel path and the lane center.

For CRCP and JPCP, six 100 mm (4-in) cores were extracted. The cores were usually taken at 90 m (300 ft) intervals, alternating between right wheel path and lane center as with HMA sampling. There were several situations in which 150 mm (6 in) cores were extracted to enable the geology crew to access the subsurface with an auger. The need to use the 150 mm (6 in) barrel was determined based on the soil sampling and testing preferences of the district geology team.

Sampling of composite pavements varied based on site conditions and specific pavement makeup. For composite sections that contained no base-mix HMA, partial depth sampling for bound asphalt and sampling for concrete were done with the 100 mm (4 in) barrel. If the pavement included an HMA base mix, at least some portion (generally partial depth) of the coring was done using the 150 mm (6 in) barrel. Generally, at least six cores spaced at 90 m (300 ft) intervals were taken from each test section. The most common approach for composite pavement sampling, however, involved eight cores spaced at 90 m (300 ft). This included two 150 mm (6 in) full-depth cores (for boring), two 100 mm (4 in) full-depth cores, and four 100 mm (4 in) cores that only extracted the HMA material.

All cores from the different sites were assessed in the laboratory by measuring their thicknesses and describing their characteristics.

In addition to the coring, subgrade soil was sampled. For each section, the local district geology crew conducted the soil investigation activities. Soil boring was confined to two core holes per test site. Some geology crews elected to use a hollow-point auger to help advance the sampling device below the bound layers: this required 150 mm (6 in) core holes. Others simply drove and extracted the sampling device directly (which could be done through the 100 mm [4 in] core hole). Continuous 0.45 m (1.5 ft) split-spoon sampling was conducted to approximately 1.35 m (4.5 ft) below the bottom of the bound material. All soil-boring activities were completed in accordance with the established VDOT procedures and field adaptations of American Society for Testing and Materials (ASTM) standard D1586 (ASTM, 2000). All soil descriptions were made in accordance with ASTM D2488 (ASTM 2000).

Laboratory Material Characterization

The bound layer materials were subjected to a detailed testing sequence to characterize their mechanical properties. This information provided complementary information about the actual condition of the materials, which was used to support the FWD analysis and is necessary for modeling the various structures investigated.

Hot mix asphalt is a viscoelastic material and as such, its deformation and recovery properties are time and temperature dependent. Creep tests in the indirect tensile (IDT) setup were performed to determine the viscoelastic properties of the material. Resilient modulus tests, also in the IDT setup, were performed in order to characterize the elastic component.

The resilient modulus test was performed in accordance with ASTM D4123 (ASTM, 1999). The test is conducted by applying a 0.1 sec pulse load followed by a 0.9 sec rest period. Tests were run for 100 cycles, of which the last five were used to calculate the resilient modulus. The applied load was chosen to induce deformations that are well above the sensitivity of the strain gauges, while at the same time minimizing damage to the specimens. The applied loads were 1000 N (224 lb) and 2000 N (449 lb) for the wearing surface and base mix layers, respectively.

The creep compliance test was run over a period of 1000 sec by applying a constant load and measuring the respective deformation. The applied loads were chosen following the same criteria as for resilient modulus. The final applied loads were 50 N (11 lb) and 100 N (22 lb) for the wearing surface and base mix layers, respectively.

Six 150 mm (6 in) cores from each section were used for testing, three for resilient modulus and three for creep. Each core provided one sample from the wearing surface and one sample from the base mix. In the cases where the wearing surface had been overlaid, the sample was taken from the most recent layer (the top). Due to the relatively thin wearing surface layer (approximately 25 mm [1 in]), it was decided to core 100 mm (4 in) diameter test specimens. The wearing surface layer was therefore cut to 25 mm (1 in) thickness, and a 100 mm (4 in) diameter specimen was cored from the cut sample. For the base mix, specimens were taken from the middle of the top base mix layer. Because the base mix layer was relatively thick, the samples were cut to 50 mm (2 in) thickness, and 100 mm (4 in) diameter specimens were then cored.

The tests were performed using an MTS servo-hydraulic machine. Horizontal and vertical deflection measurements were taken over a 25 mm (1 in) gauge length on both sides of the specimen. The data collected include the applied load and the horizontal and vertical deformations. All tests were performed at 25 ^{o}C (77 ^{o}F). Specimens were stored in the laboratory at room temperature (25 ^{o}C). Before being tested, specimens were placed in an environmental chamber at 25 ^{o}C (77 ^{o}F) for a period of 1 hour. Typical measured deformations during the resilient modulus and the creep tests are presented in Figure 3 and Figure 4, respectively.

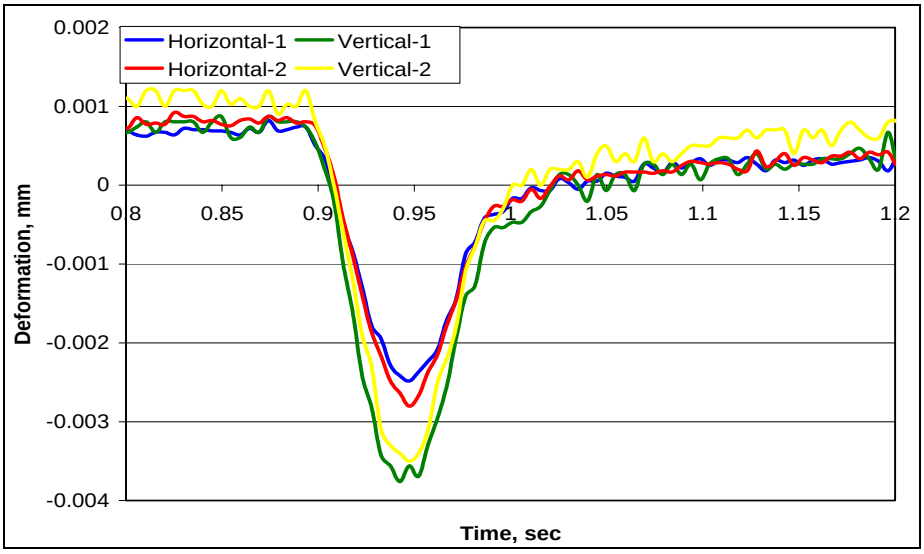

Figure 3. Measured deformations during a resilient modulus test

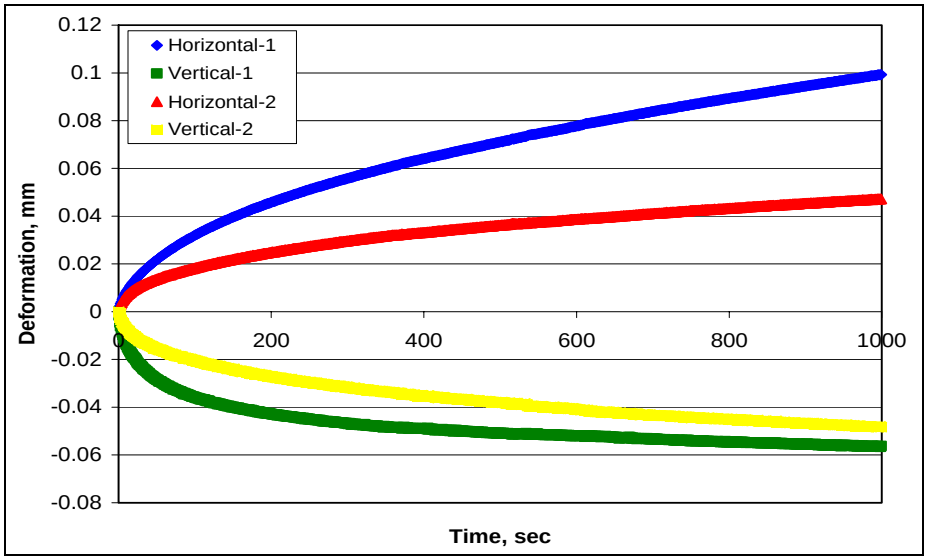

Figure 4. Measured deformations during a creep test

For concrete, unconfined compressive strength in accordance with ASTM C39/C39M-99 (ASTM, 1999) was performed on two cores per site. The cores were cut to a height of 203 mm (8 in) prior to testing. A Forney machine was used to perform the tests.

Smoothness, Rutting, and Friction

Smoothness and friction of the pavement sections was measured to determine and compare the functional quality of the pavement at the various sites. These two parameters are important condition indicators since they reflect the two main concerns of the road users.

The smoothness and rutting were measured using VDOT's laser-based ICC profiler during the months of October and November 2004. The profiler uses a short-range laser range finder, an accelerometer, and a distance measuring transducer to measure and compute the roadway profile. The profile is converted into an International Roughness Index (IRI) in accordance with ASTM E1926 (ASTM, 1998).

Wet pavement friction was measured with an ASTM skid trailer using a smooth tire (ASTM E524) in accordance with ASTM E274 (ASTM, 2000). All tests used a target speed of 64 km/hr (40 mph).

RESULTS AND DISCUSSION

GPR Testing

Samples of the raw GPR data collected from a flexible section, a CRCP section, a JPCP section, and a composite section are depicted in Figure 5 through Figure 8, respectively. These figures show a Linescan (or B-scan) view of the data, which represents GPR scans stacked together vertically with their reflection amplitudes color-coded according to the amplitude-to-color transform functions shown on the right of the figures. The *x*-axis in these figures represents the survey distance along the tested section. The *y*-axis represents the two-way time of travel (in nanoseconds) of the electromagnetic (EM) waves between the different layer interfaces.

The two-way time of travel may be converted to layer thicknesses after estimating the dielectric constants of the different layers detected within the pavement section. As can be seen in these figures, the raw data give only the approximate locations of the major layer interfaces (in time-delay units) and not the actual layer thickness.

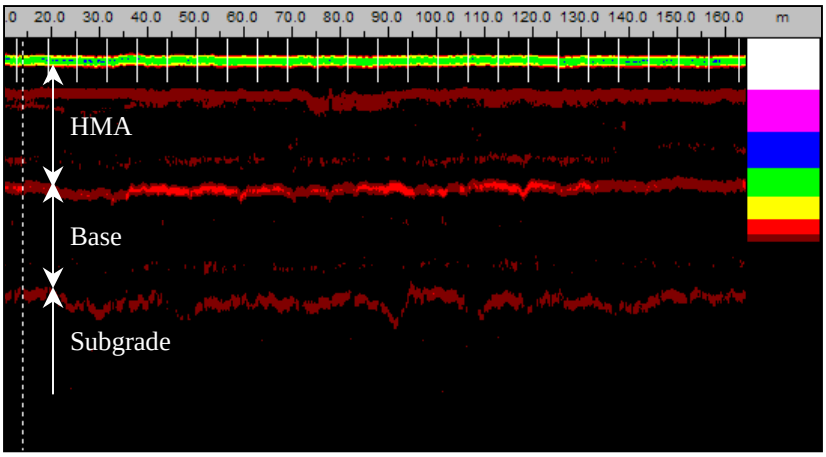

Figure 5. Raw GPR data, Site 03, center of the lane, flexible pavement

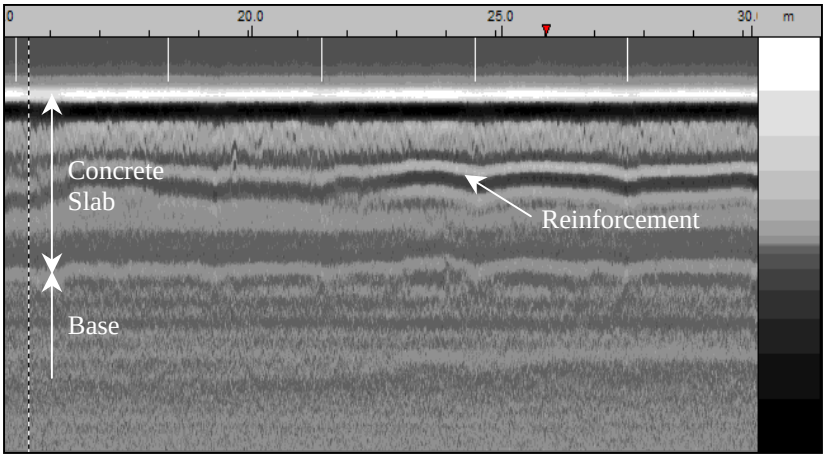

Figure 6. Raw GPR data, Site 04, center of the lane, CRCP

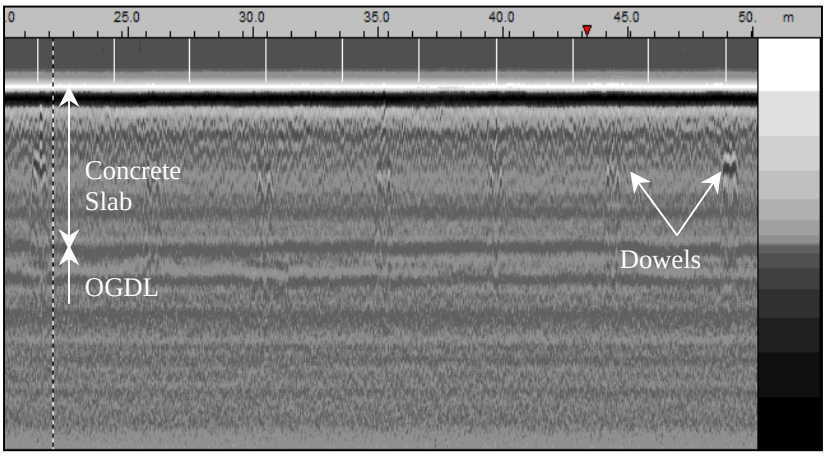

Figure 7. Raw GPR data, Site 07, center of the lane, JPCP

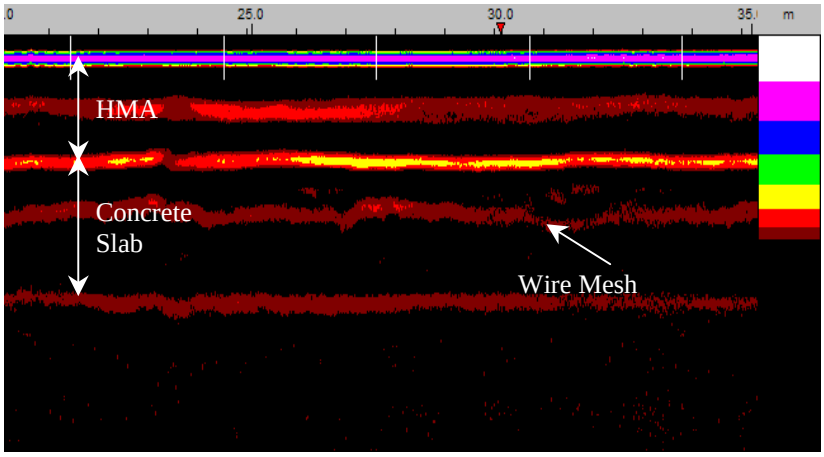

Figure 8. Raw GPR data, Site 08, center of the lane, composite pavement

The collected GPR data were analyzed to provide the thickness variations of the different layers composing each pavement section. For all sites, the layer thicknesses were estimated along the center of the lane and the right wheel path (left wheel path for Site 18) at a spacing of 0.3 m (1 ft) starting from the beginning of the Site.

Figure 9 and Figure 10 shows the GPR thickness results for the detected layers from Site 01 at the center of the lane and at the right wheel path, respectively. For comparison purposes, the thickness measured directly on the cores taken from the different sites are also depicted in these figures at their respective locations. Detailed layer thickness results for all the tested sites are available from the authors.

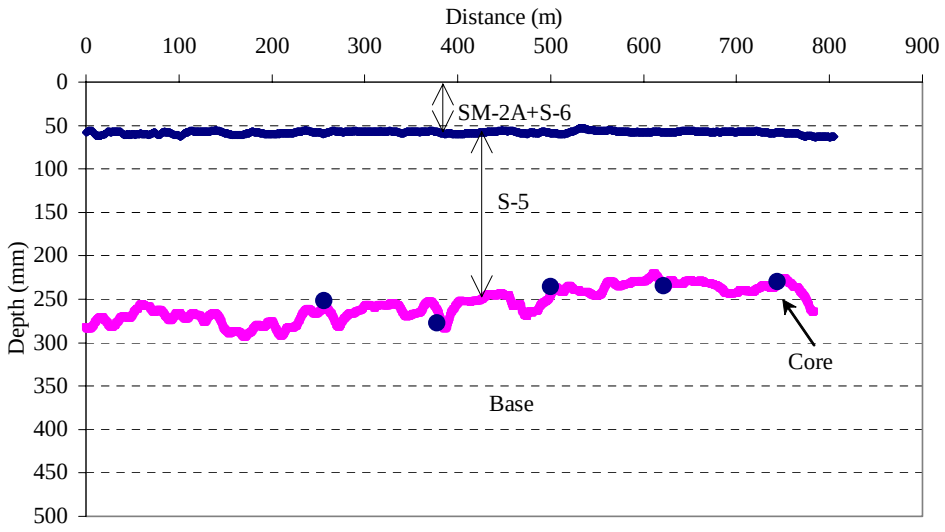

Figure 9. Layers' thicknesses for Site 01 (lane center)

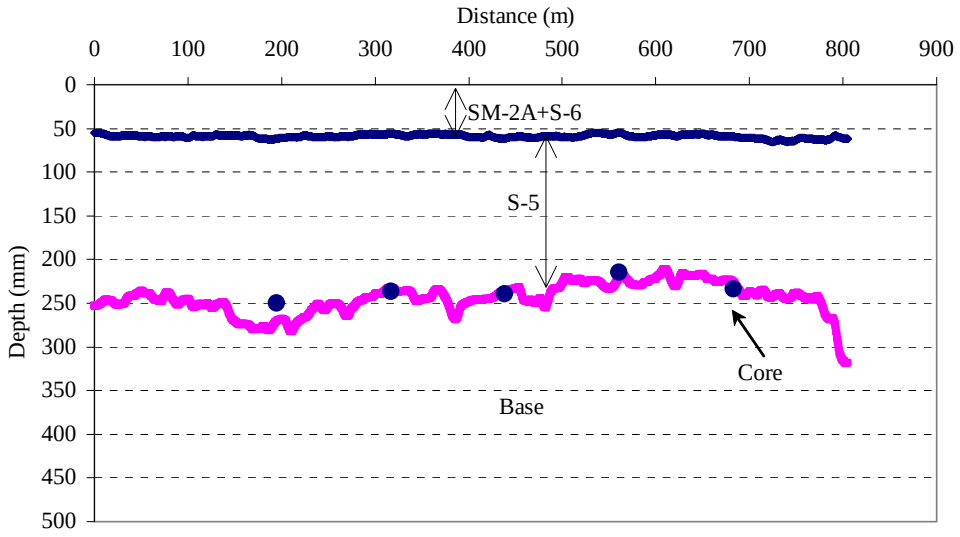

Figure 10. Layers' thicknesses for Site 01 (right wheel path)

It should be noted that depending on the pavement structure (flexible, rigid, or composite) and the dielectric constant contrast between the materials of the adjacent layers, some layers were not detected from the GPR data. In particular, the different layers of the following pavement configurations were not entirely resolved from the GPR data in many sites:

1. Different types of thin HMA layers (as in the case of SM-2A on top of S-6 in Site 01).
2. Base layer and subgrade composed of materials having comparable dielectric constants (as in the case of Site 01).
3. Interface between the concrete slab and the sub-base layer especially in the composite sections (as in the case of Site 02).
4. Other layers underneath the concrete slab in a JPCP, CRCP, or composite pavement (as in Site 07).

The accuracy of the GPR results was estimated by comparing the thickness determined from the stationary GPR data taken at the core locations to the thickness measured directly on the cores. The stationary GPR data taken near the core locations were analyzed by the same software and the same procedure as the other GPR data. Because it is usually difficult to accurately measure the thickness of the individual layers composing a core (especially for HMA cores where the layer limits are sometimes not easily separable), the GPR thickness error were estimated based on the thickness of the whole cores.

The estimated average GPR thickness errors found for all the sites are summarized in Figure 11. According to these results, the average absolute thickness error varied between 1.8% for Site 04 to 8.4% for Site 16. The average absolute GPR thickness error for all sites was approximately 4.7%. It should be mentioned that for the composite sections, the GPR error was estimated for the HMA layers only due to the unavailability of the thickness of the concrete slab

either from the cores or from the GPR data. The concrete thickness could not be determined from the GPR data in the case of composite pavements if its bottom interface produced a very low reflection that was not detected by the GPR receiver.

Finally, it is worth noting that the errors found for some sites (such as Sites 06 and 16) were due to several factors including:

1. Sometimes the cores were not taken at the exact same locations where the GPR data were collected because of the difficulties encountered in positioning the coring machine.
2. For the flexible sites that had an open-graded drainage layer OGDL layer (such as Site 12 and Site 18), the thickness of the HMA OGDL layer was usually incorporated in the GPR HMA thickness because it was difficult to separate the layers.
3. Inaccuracy of the thicknesses of the HMA cores, especially if the HMA layer is placed on a base layer that has relatively large aggregates made it difficult to determine the exact location of the interface between the HMA and the base.
4. Broken cores made it difficult to measure accurate layer thicknesses.
5. The system cannot separate the reflections resulting from distinct adjacent layers with comparable dielectric constants, which results in using an erroneous dielectric constant for computing the layer thicknesses. This situation is usually encountered for very old pavements having many thin overlays of different ages (such as in Sites 01, 02, 05, 15, 16, and 17).

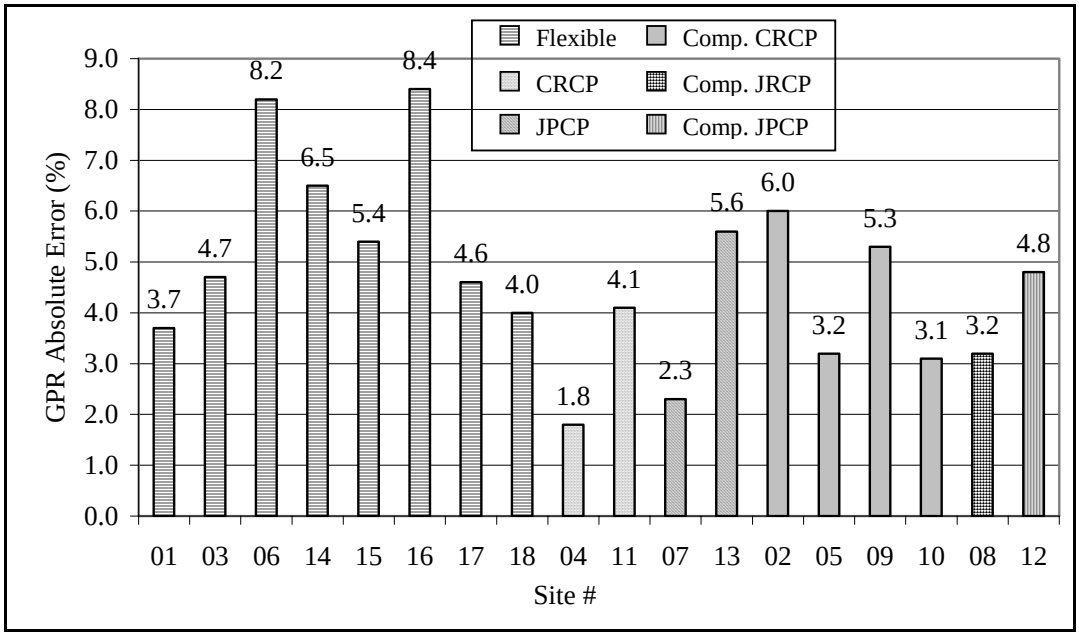

Figure 11. Average GPR absolute thickness error per site

FWD Testing

The *in situ* elastic moduli for all pavement layers were backcalculated from the measured deflections. The results presented in this report are based on a load level of 40 kN (9000 lb). The backcalculation procedure involved calculating theoretical deflections under the applied load using assumed pavement layer moduli. These theoretical deflections were then adjusted in an iterative process until the theoretical and measured deflection basins reach an acceptable agreement and reasonable backcalculated modulus for each layer were obtained. Backcalculated results were compared to typical values obtained from experience or historical records (see Table 2) to identify weak material layers and to determine current structural adequacy.

Many backcalculation software packages are currently available; however, most of them are specially designed to analyze flexible pavements, making it difficult to find a suitable backcalculation software package to evaluate composite and rigid pavements. The software package used for the backcalculation process was ELMOD version 5.1, developed by Dynatest. ELMOD's approach is based on the Odemark-Boussinesq Method of Equivalent Thickness (MET).

Table 2. Typical stiffness moduli for different materials

Material	Initial Modulus, MPa (ksi)	Range of values, MPa (ksi)	
		Low	High
Asphalt Materials			
Hot Mix Asphalt	3500 (500)	2000 (300)	5500 (800)
PCC Materials			
Intact slab	31000 (4500)	20500 (3000)	41500 (6000)
Fractured slab	3500 (500)	700 (100)	20500 (3000)
Open Grade Drainage Layers			
Asphalt Stabilized	1000 (150)	700 (100)	1700 (250)
Cement Stabilized	1700 (250)	1000 (150)	2400 (350)
Cement Stabilized Layers			
Cement Treated Aggregate	5800 (850)	4800 (700)	13800 (2000)
Stabilized Subgrade	2400 (350)	900 (130)	3800 (550)
Unbound Materials			
Crushed stone/gravel, Base	350 (50)	70 (10)	1000 (150)
Gravel or soil-agg. mix, coarse Base	200 (30)	70 (10)	700 (100)
Gravel or soil-agg. mix, fine Base	150 (20)	35 (5)	550 (80)

In addition to ELMOD, another software package called TAG (Total Analysis Group) was used. TAG was developed by the VDOT to analyze FWD data, and it was utilized in this project to obtain homogeneous sections for the pavement structures. Obtaining the cumulative sums of deflection allows the division of each project into sections with similar performance.

Figure 12 illustrates the homogeneous sections obtained for Site 02. Two sensors were selected to obtain homogeneous sections: (a) maximum deflection (sensor at 0 mm from loading plate center); and (b) Sensor 7 (sensor at 1219 mm from loading plate center). Sensor 7 was selected instead of Sensor 9 because the cumulative sums of deflection of the last sensor tend to be too flattened thus the changes in the homogeneous sections cannot easily be identified.

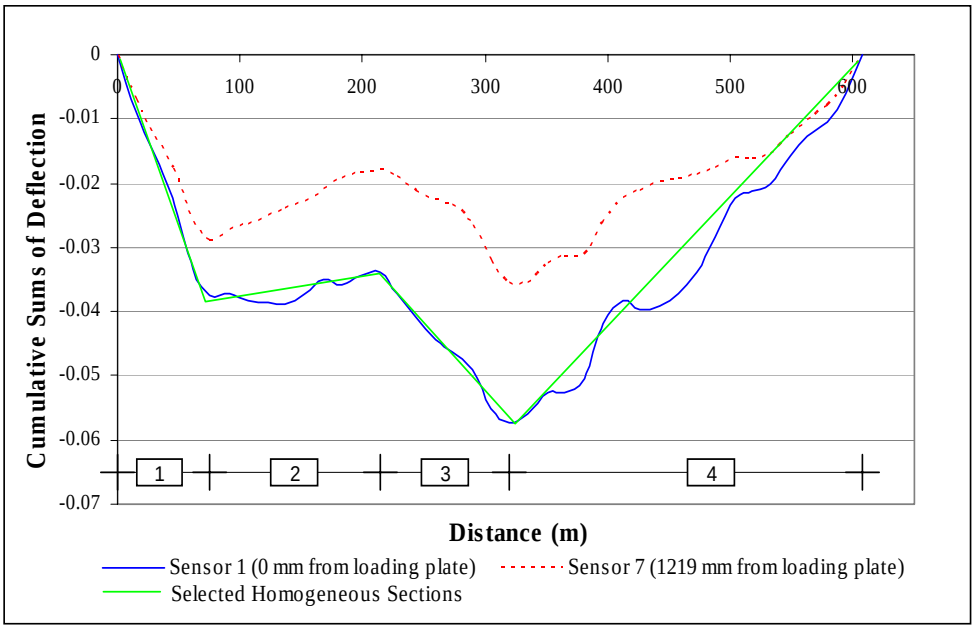

Figure 12. Homogeneous sections based on cumulative sums of deflection (Site 02)

The backcalculation results obtained for each pavement structure do not show significant differences between each homogeneous section. This is possibly because the length of each pavement section is only 800 m and the coefficient of variation (COV) within measured deflections is generally between low and average, as shown in Table 3 for geophones 1 (maximum deflection), 7, and 9 (subgrade deflection). The only exception for this situation is Site 03, where similar results were obtained for the base layer in sections 1 and 3 and different results were noted for section 2.

Three sources of information were compared to obtain accurate layer thickness: (a) historical data; (b) GPR ; and (c) measured cores. Given that some of the historical data obtained for a few projects was inaccurate, missing, or not updated, the most reliable source for layer thickness was considered to be the cores, which were subsequently compared to GPR results, followed by the historical data. Tables containing layer thickness comparisons for all tested sites are available from the authors

Backcalculation results are summarized in Table 4 through Table 7. It is important to mention that for the flexible and composite sites, the wearing surface and HMA base mix layer were considered as one layer. This was done because it is not recommended to separate HMA layers with a thickness less than 75 mm.

Table 3. Deflection variability expressed in terms of coefficient of variation

Site #	Ave. D1 μm (mils)	COV* (%)	COV level+	Ave. D7 μm (mils)	COV (%)	COV level+	Ave. D9 μm (mils)	COV* (%)	COV level+
FLEXIBLE PAVEMENTS									
01	156 (6.1)	25	A	57 (2.2)	27	A	33 (1.3)	30	A
03	98 (3.9)	47	H	43 (1.7)	56	H	18 (0.7)	68	H
06	185 (7.3)	15	L	29 (1.1)	22	L	18 (0.7)	21	L
14	91 (3.6)	20	L	16 (0.6)	36	A	10 (0.4)	42	H
15	200 (7.9)	10	L	38 (1.5)	17	L	21 (0.8)	20	L
16	94 (3.7)	16	L	23 (0.9)	32	A	13 (0.5)	35	A
17	149 (5.9)	16	L	35 (1.4)	21	L	22 (0.9)	25	A
18	89 (3.5)	18	L	24 (0.9)	32	A	16 (0.6)	37	A
COMPOSITE PAVEMENTS									
02	96 (3.8)	14	L	44 (1.7)	21	L	30 (1.2)	24	A
05	106 (4.2)	18	L	46 (1.8)	31	A	32 (1.2)	33	A
08	278 (10.9)	34	A	122 (4.8)	37	A	84 (3.3)	38	H
09	96 (3.8)	25	A	37 (1.5)	23	A	26 (1.0)	22	L
10	66 (2.6)	14	L	28 (1.1)	13	L	19 (0.8)	12	L
12	58 (2.3)	13	L	18 (0.7)	14	L	14 (0.5)	17	L
CRCP									
04	124 (4.9)	18	L	61 (2.4)	24	A	39 (1.5)	25	A
11	50 (2.0)	17	L	28 (1.1)	22	L	19 (0.8)	21	L
JCP									
07	56 (2.2)	56	H	21 (0.8)	21	L	18 (0.7)	15	L
13	39 (1.5)	13	L	29 (1.2)	15	L	18 (0.7)	15	L

* COV = Coefficient of Variation = (standard deviation/average) * 100

+ COV Level: Low ~ 15% (COV< 22.5%); Average ~ 30% (22.5%≤COV<37.5%); High ≅ 45% (37.5%≤COV)

Table 4. Summary of backcalculation results for flexible pavements

MATERIAL	Pav. Temp., °C (°F)	Backcalculated Moduli, MPa (ksi)			RMS
		Average	Std. dev.	COV	
SITE 01					
SM + BM	23.4 (74.2)	3185 (462)	986 (143)	31%	3.21
Cement Treated Aggregate	-	8660 (1256)	3627 (526)	42%	
Subgrade	-	110 (16)	34 (5)	31%	
SITE 03					
Sections 1 & 3					
SM+BM	17.4 (63.4)	3723 (540)	1282 (186)	34%	4.04
Base	-	2958 (429)	1172 (170)	40%	
Subgrade	-	248 (36)	110 (16)	44%	
Section 2					
SM+BM	21.4 (70.6)	3840 (557)	1213 (176)	32%	2.47
Base	-	427 (62)	131 (19)	31%	
Subgrade	-	97 (14)	41 (6)	42%	
SITE 06					
SM + BM	22.7 (72.9)	1593 (231)	262 (38)	16%	4.39
#22 Aggregate	-	276 (40)	76 (11)	28%	
Cement Stabilized Subgrade (10%)	-	2634 (382)	786 (114)	30%	
Subgrade	-	276 (40)	69 (10)	25%	
SITE 14					
SM + BM	32.0 (89.6)	3599 (522)	800 (116)	22%	4.61
Asphalt Stab. OGDL	-	1413 (205)	345 (50)	25%	
Cement Stabilized Aggregate	-	2834 (411)	752 (109)	26%	
Subgrade	-	469 (68)	138 (20)	29%	
SITE 15					
SM + BM	23.2 (73.8)	1834 (266)	296 (43)	16%	5.06
Agg. Base Type I + Select Material Type I	-	276 (40)	62 (9)	23%	
Subgrade	-	145 (21)	28 (4)	20%	
SITE 16					
SM + BM	18.4 (65.2)	4013 (582)	614 (89)	15%	2.97
Agg. Base Type I + Select Material Type I	-	683 (99)	152 (22)	22%	
Subgrade	-	248 (36)	76 (11)	29%	
SITE 17					
SM + BM	20.6 (69.1)	2779 (403)	510 (74)	18%	4.13
Subgrade	-	207 (30)	48 (7)	22%	
SITE 18					
SM + BM	25.8 (82.8)	3909 (567)	724 (105)	19%	3.06
Asphalt Stab. OGDL Type I (2%)	-	1207 (175)	276 (40)	23%	
21B	-	634 (92)	138 (20)	22%	
Subgrade	-	317 (46)	103 (15)	32%	

Table 5. Summary of backcalculation results for composite pavements

MATERIAL	Pav. Temp.*, °C (°F)	Backcalculated Moduli, MPa (ksi)			RMS
		Average	Std Dev	COV	
SITE 02					
SM + BM	28.2(82.7)	2337 (339)	483 (70)	21%	1.64
CRCP	-	31785 (4610)	8294 (1203)	26%	
Subgrade	-	262 (38)	62 (9)	23%	
SITE 05					
SM + BM	18.1(64.6)	2544 (369)	324 (47)	13%	2.78
CRCP	-	26834 (3892)	6729 (976)	25%	
Aggregate #22	-	469 (68)	131 (19)	28%	
Subgrade	-	241 (35)	69 (10)	29%	
SITE 08					
SM + BM	20.8 (69.4)	1462 (212)	538 (78)	37%	4.01
JRCP	-	10266 (1489)	4992 (724)	49%	
Subgrade	-	90 (13)	21 (3)	20%	
SITE 09					
SM + BM	30.1 (86.1)	1841 (267)	945 (137)	51%	2.95
CRCP	-	15851 (2299)	6233 (904)	39%	
Cement Treated Aggregate	-	2282 (331)	979 (142)	43%	
Subgrade	-	296 (43)	62 (9)	22%	
SITE 10					
SM + BM	20.0 (68)	3958 (574)	179 (26)	5%	2.75
CRCP	-	17844 (2588)	7467 (1083)	42%	
Cement Treated Aggregate	-	3723 (540)	945 (137)	25%	
Subgrade	-	365 (53)	55 (8)	15%	
SITE 12					
SM + BM	20.6 (69)	4095 (594)	793 (115)	19%	1.97
Asphalt Stabilized OGDL	-	779 (113)	269 (39)	34%	
JPCP	-	25000 (3626)	7260 (1053)	29%	
Cement Stabilized Subgrade + Subgrade	-	586 (85)	90 (13)	15%	

Table 6. Summary of backcalculation results for CRCP

MATERIAL	Backcalculated Moduli, MPa (ksi)			RMS
	Average	Std. Dev	COV	
SITE 04				
CRCP	27800 (4032)	3799 (551)	14%	1.35
21A 4%	689 (100)	248 (36)	37%	
Cement Stab. Subgrade 10%	324 (47)	97 (14)	31%	
Subgrade	131 (19)	34 (5)	25%	
SITE 11				
CRCP	29806 (4323)	6778 (983)	23%	2.16
Cement OGDL Type I (6.25%)	1469 (213)	372 (54)	25%	
21A 4%	4888 (709)	724 (105)	15%	
Subgrade	365 (53)	97 (14)	26%	

Table 7. Summary of backcalculated results for JPCP

MATERIAL	Backcalculated Moduli, MPa (ksi)			RMS
	Average	Std. Dev	COV	
SITE 07				
JPCP	22504 (3264)	17051 (2473)	76%	6.35
Asphalt OGDL Type 1 3%	1000 (145)	593 (86)	59%	
21A	4109 (596)	2661 (386)	65%	
Subgrade	469 (68)	83 (12)	18%	
SITE 13				
JPCP	42823 (6211)	6405 (929)	15%	2.57
Asphalt Stab. OGDL Type 1	648 (94)	386 (56)	60%	
21A 4%	3282 (476)	1020 (148)	31%	
Cement Stabilized Soil (10%)	848 (123)	441 (64)	52%	
Subgrade	386 (56)	83 (12)	21%	

In general, composite CRCP and JPCP projects are complex pavement structures, which are difficult to model with any backcalculation program. Some studies have shown that the Method of Equivalent Thickness may produce erroneous results for these cases. These structures violate some of the assumptions of the model used (e.g. moduli not decreasing monotonously with depth). In addition, backcalculation software may overestimate the modulus of the rigid layers and subsequently underestimate those of other layers, or vice versa. In these cases, the goodness of fit should not be the only determining factor in selecting the best model. Despite these limitations, the obtained results for most of the sections were considered reasonable.

Figure 13 through Figure 15 illustrate the backcalculation results for typical flexible, composite and CRCP pavements, respectively. These figures show the estimated moduli for each layer. Results from laboratory tests, performed on some of the HMA and concrete cores, were also presented in these figures. Results for all other sites are available from the authors.

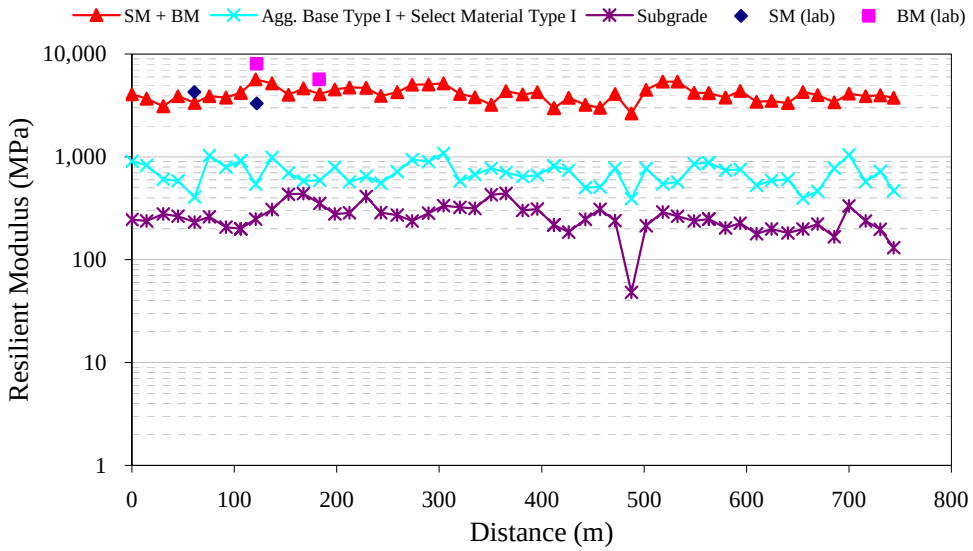

Figure 13. Backcalculation results, Site 16 (flexible)

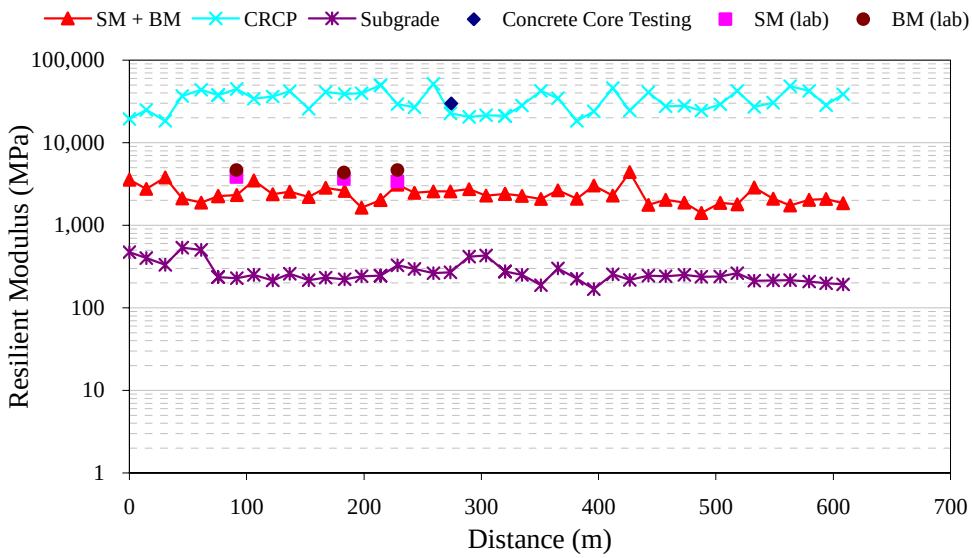

Figure 14. Backcalculation results, Site 02 (composite)

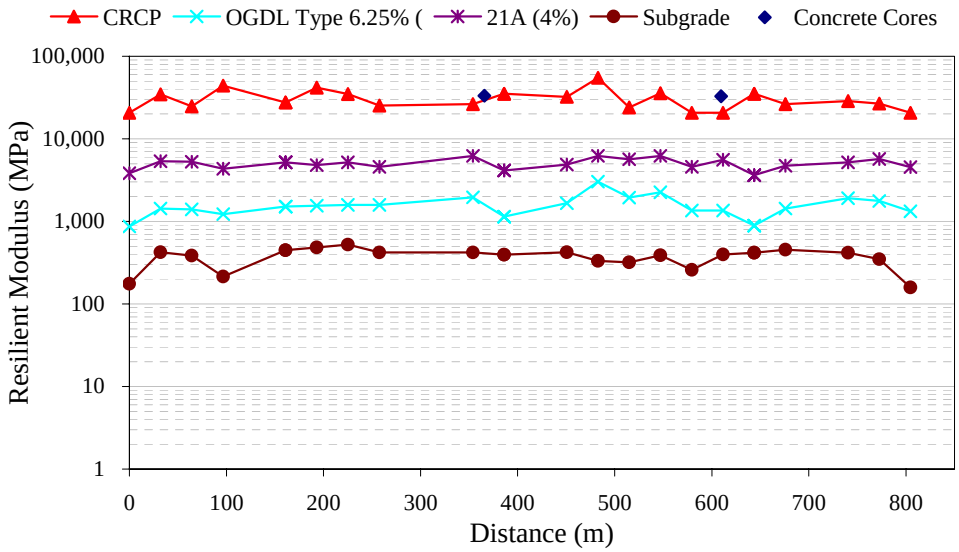

Figure 15. Backcalculation results, Site 11 (CRCP)

Visual/Video Survey

Existing pavement distresses were extracted from the digital videos using the procedure recommended by the VDOT Distress Rating Manuals (VDOT, 2001, 2002). The procedure followed is consistent with the methodology used by VDOT for determining the condition indices used for planning pavement maintenance and rehabilitation activities on a project basis. These indices are also used by the central office pavement management personnel to describe network level pavement condition, optimization, and other studies directed at the best use of available funds.

The procedure adopted for flexible and composite pavements determines the condition of the road according to two major indices: the Load-Related Distress Rating (LDR), which considers distresses caused by traffic loads (alligator cracking, rutting, and patching); and the Non-Load-Related Distress Rating (NDR), which considers distresses due to temperature and moisture changes and other climate-related issues (e.g., reflection cracking, transverse cracking, and patching). Both indices range from a value of 100 for a pavement in perfect condition to a value of 0 for a very poor pavement. The overall condition of the pavement is reported as the lower of the two indices (LDR or NDR), referred to as the Critical Condition Index (CCI).

For the rigid pavements, because of the need to consider maintenance and rehabilitation options separately for jointed and continuously reinforced pavements, the indices available were the slab distress rating (SDR) and the joint faulting index (JFI) for jointed pavements and the concrete distress rating (CDR) and the concrete punch-out rating (CPR) for CRCP. The overall condition of the pavement is also reported as the lower of the two indices, referred to as the CCI. The JFI was not computed because faulting information was not collected.

Rutting was measured with the profiler as is discussed later. All the other distress types were evaluated based on the collected digital videos. Samples of alligator cracking, patching, and transverse cracking observed in some of the sites are presented in Figure 16 through Figure 18, respectively. The resulting CCI found for all sites having an asphalt wearing surface (i.e., flexible and composite) are presented in Table 8, and the results for the rigid pavements are in Table 9 and Table 10.

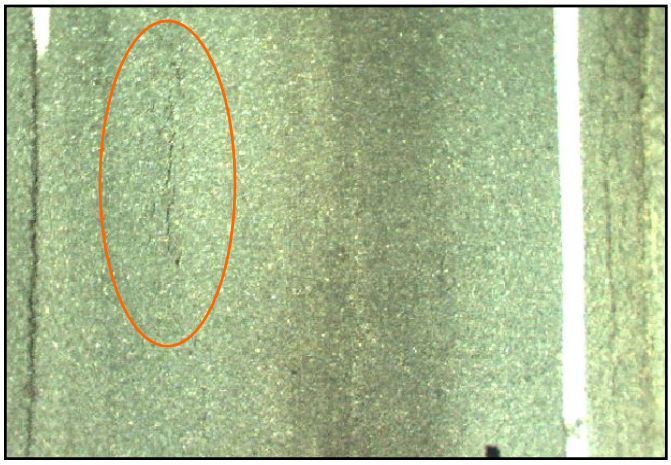

Figure 16. Example of low severity alligator cracking

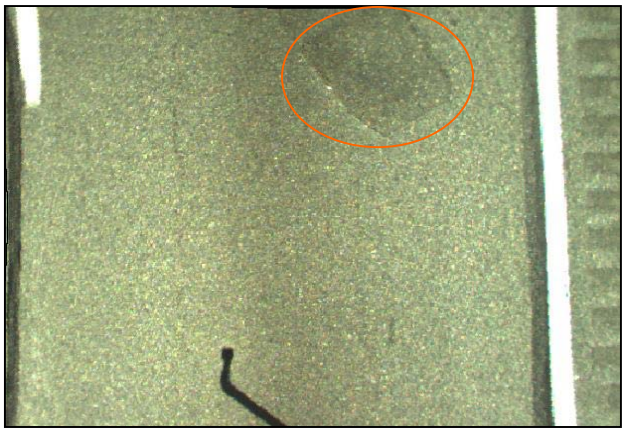

Figure 17. Example of patching

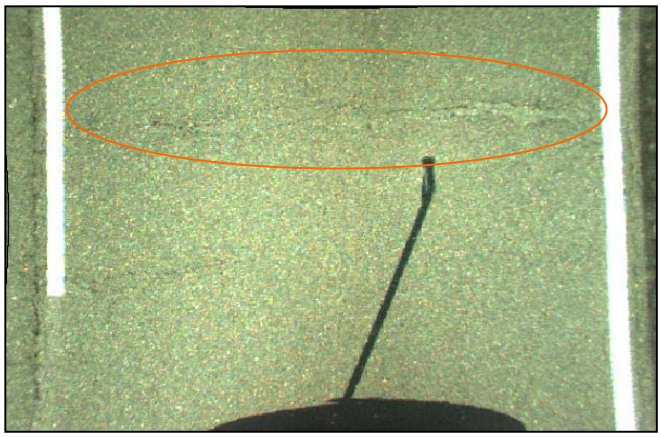

Figure 18. Example of transverse cracking

Table 8. Flexible and composite pavements' condition results

Site	Cracking (ft)							Patch (#)	Pot. (#)	Del.	Rut Depth (in)	NDR	LDR	CCI
	Longitudinal		Transversal		Fatigue									
	1	2	1	2	L	M	S							
01	58	178	48	264	160	0	0	0	0	0	0.12	74.5	96.7	**75**
02	120	85	84	6	9	0	0	0	0	0	0.22	87.5	86.7	**87**
03	0	112	440	338	170	0	0	0	0	0	0.13	68.6	95.8	**69**
05	264	25	48	72	129	0	0	9	0	0	0.27	88.1	77.3	**77**
06	21	29	90	276	93	18	0	0	0	0	0.13	80.5	96.3	**81**
08	132	0	0	0	0	0	0	0	0	0	0.0	97.3	100	**97**
09	136	95	12	144	25	0	0	0	0	0	0.02	83.1	99.7	**83**
10	39	14	24	0	4	0	0	0	0	0	0.04	97.8	100	**98**
12	130	3	0	0	0	0	0	0	0	0	0.15	97.2	95.8	**96**
14	4	0	0	0	5	0	0	0	0	0	0	99.9	99.9	**100**
15	112	86	0	0	0	0	0	0	0	0	0.20	92.3	89.7	**90**
16	61	112	12	0	14	0	0	0	0	0	0.03	91.6	99.8	**92**
17	216	0	240	0	540	0	0	0	0	0	0	92.0	94.2	**92**
18	0	0	0	0	0	0	0	0	0	0	0	100	100	**100**

Table 9. Jointed PCC pavements' condition results

Site	Corner Breaks	Transv. Joint Spalls	Long. Joint Spalls	Cracking.		Divided Slabs	PCC Patch	AC Patch	SDR	JFI	CCI
				Transv.	Long.						
07							72 ft^2 2/181		99.8	N/A	**100**
13		2/136 S1			2/136 S1				97.1	N/A	**98**

Table 10. CRC Pavements' Condition Results

Site	Punch outs	Cluster Cracking	AC Patch	PCC Patch	Cracking.		Long Joint Spalls	CPR	CDR	CCI
					Transv.	Long.				
04	86 ft^2		3 ft^2		774 S1 252 S2 240 S3	32 ft^2		98.7	99.8	**99**
11	87 ft^2		48 ft^2	60 ft^2 S1 & 180 ft^2 S3	1,956 S1 3,696 S2 2,304 S3	32 ft^2		98.3	98.9	**98**

Key:

- LDR: Load Related Distress Index
- NDR: Non-load Related Distress Index
- SDR: Slab Distress Rating
- CDR: Concrete Distress Rating
- CPR: Concrete Punchout Rating
- CCI: Critical Condition Index

For the flexible and/or composite pavements, there were almost no problems with reflective cracking and/or fatigue cracking above severity level 1. However, sites that exhibited high levels of severe transverse cracking (01, 03 and 05) and high rutting (02 and 04) had the lowest condition ratings. Site 09 had a good share of most distresses giving it a low score also.

All of the rigid pavements evaluated did not show any significant extent of distresses, which shows in the high scores obtained for all of them.

Laboratory Material Characterization

The average resilient modulus results for the tested HMA layers are presented in **Table 11**. Reported is the average resilient modulus for the wearing surface and base mix.

The wearing surface resilient modulus varied between 2,792 and 6,722 MPa (405 and 975 ksi) with an average of 4,723 MPa (685 ksi). The values for the base mixes varied between 2,951 and 6,846 MPa (428 and 993 ksi) with an average of 4,448 MPa (651 ksi).

Figure 19 shows the creep compliance results for the wearing surface mix of Site 05. Results for all the other sites are available from the authors.

Table 11. Resilient modulus results

Site #	Wearing Surface		Base Mix	
	Average, MPa (ksi)	COV (%)	Average, MPa (ksi)	COV (%)
01	5143 (746)	7.7	2985 (433)	26.5
02	4488 (651)	6.0	3654 (530)	21.6
03	6157 (893)	16.0	4854 (704)	19.0
05	5371 (779)	15.8	4378 (635)	27.7
06	3730 (541)	51.8	2951 (428)	3.9
08	2420 (351)	49.9	NA	NA
09	6722 (975)	31.1	NA	NA
10	3006 (436)	11.0	4144 (601)	15.0
12	5205 (755)	31.4	6640 (963)	36.7
14	4392 (637)	32.0	4095 (594)	31.0
15	6343 (920)	7.6	3337 (484)	9.0
16	4206 (610)	32.0	6846 (993)	51.0
17	4433 (643)	15.7	4522 (656)	18.2
18	4136 (600)	38.0	4971 (721)	51.0

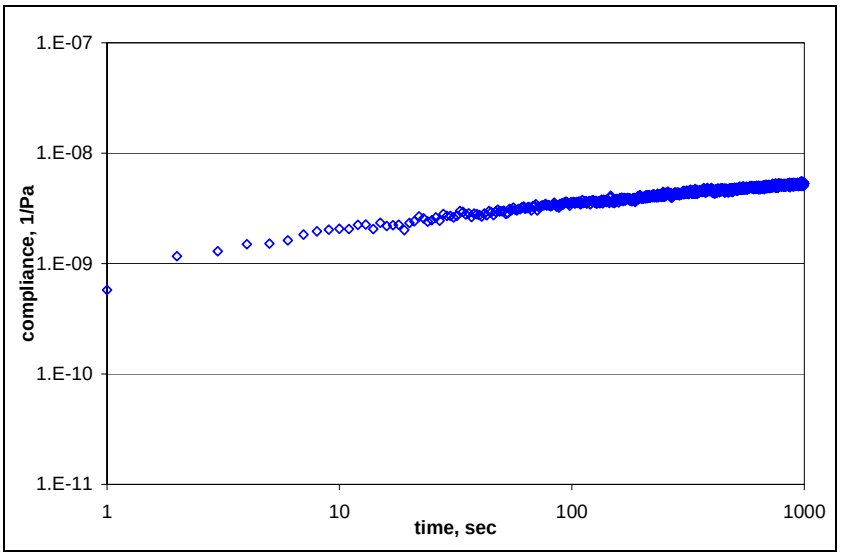

Figure 19. Creep compliance for Site 05 (wearing surface)

Characterization of the viscoelastic properties for HMA surface and base mixes was performed by fitting a Prony series expansion to the measured creep data. The Prony series (Generalized Kelvin model), in general, adequately describes the material response with respect to time and is given by the following equation:

$$D(t) = D_0 + \sum_{i=1}^{N} D_i (1 - e^{-t/\tau_i}) \quad (1)$$

where
D(t) = creep compliance at time t; and
D_i (Prony series coefficients) and τ_i (retardation times) = material constants.

To obtain the material constants in Equation 1, a number of Prony series terms were assumed to cover the considered time span, and the fitting process was then conducted using nonlinear regression to find the retardation times and the coefficients of the Prony series using the SAS statistical package. In general, three to four Prony series terms were used to obtain an accurate fit (see Figure 20 for illustration). The fitted creep compliance was then used to predict the relaxation modulus, E(t), by using Equation 2 (Kim *et al.*, 2002):

$$E(t)\,D(t) = \frac{\sin n\pi}{n\pi} \tag{2}$$

where n = positive constant, obtained by fitting a localized power law model ($D(t) = D_1 t^n$) to the different regions of behavior.

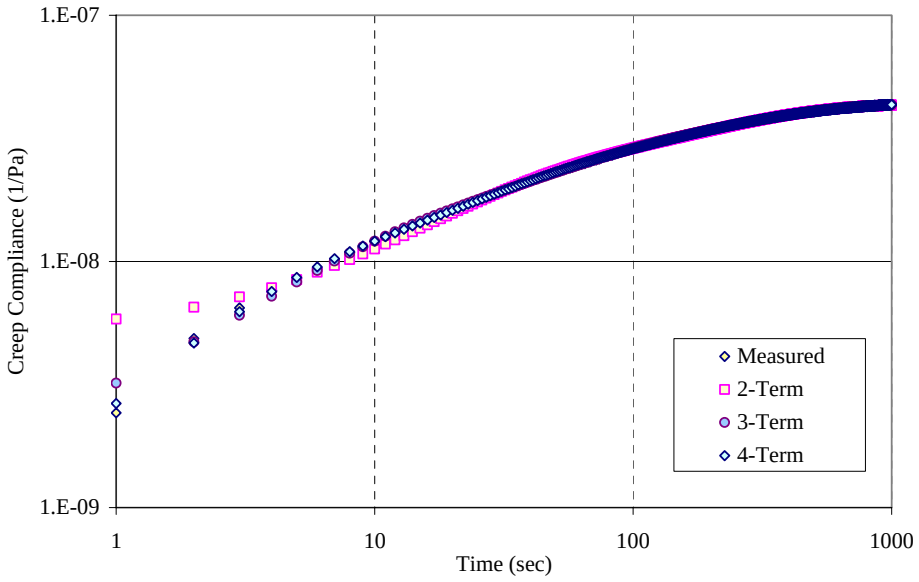

Figure 20. Comparison between measured and calculated creep compliance for different Prony series

Similarly, a Prony series function was fitted to the relaxation modulus variation with time. Then, the bulk [K(t)] and shear [G(t)] moduli variation with time were estimated using the following relations assuming that Poisson's ratio (ν) does not change with time:

$$K(t) = \frac{E(t)}{3(1-2\nu)} \tag{3}$$

$$G(t) = \frac{E(t)}{2(1+\nu)} \tag{4}$$

Based on this process, characterization of the viscoelastic properties of HMA was completed at a reference temperature of 25 °C (77 F) and all required material parameters were defined.

Results of the compressive strength of concrete are shown in Table 12. This data were used to find the elastic modulus of concrete using the correlation equation:

$$E_c = 57000\left(f_c\right)^{0.5} \quad (5)$$

where
E_c = modulus of elasticity (psi); and
f_c =concrete compressive strength (psi).

Table 12. Compressive strength and estimated modulus of concrete cores

Site #	Avg. Comp. Strength, MPa (psi)	COV (%)	Estimated Modulus, MPa (ksi)
02	40.9 (5930)	4.3	30,273 (4391)
04	51.5 (7470)	NA	33,970 (4927)
05	48.2 (6990)	8.1	32,864 (4767)
07	52.8 (7660)	3.0	34,396 (4989)
08	62.2 (9020)	3.2	37,332 (5415)
09	57.3 (8310)	NA	35,832 (5197)
10	36.1 (5240)	NA	28,441 (4125)
11	48.7 (7060)	1.4	33,034 (4791)
13	56.8 (8240)	3.7	35,675 (5174)

Smoothness and Friction

The average roughness, rutting, and skid number values measured for each site are summarized in Table 13. With a few exceptions, all the sites exhibit adequate ride quality. Sites 01, 04, and 13 have the highest IRI. All collected data are available from the authors.

Table 13. Roughness for the measured sites

Site #	Type	Roughness, IRI mm/km (in/mi)	IRI COV (%)	Rutting mm (in)	Skid Number SN40	SN40 COV (%)
01	Flexible	1529.4 (96.9)	33.1	3.0 (0.12)	37.9	9.1
02	Comp.	1374.7 (87.1)	17.7	5.6 (0.22)	32.7	7.0
03	Flexible	1202.7 (76.2)	28.7	2.8 (0.11)	39.9	3.5
04	CRCP	1537.2 (97.4)	27.9	2.3 (0.09)	37.5	10.1
05	Comp.	1188.4 (75.3)	30.2	6.6 (0.26)	45.9	4.6
06	Flexible	1005.4 (63.7)	28.7	3.3 (0.13)	44.4	4.3
07	JPCP	888.6 (56.3)	39.4	0.5 (0.02)	35.1	33.1
08	Comp.	1139.5 (72.2)	38.5	0.0 (0.00)	45.2	4.2
09	Comp.	1306.8 (82.8)	29.0	1.3 (0.05)	37.0	4.1
10	Comp.	1041.7 (66.0)	21.6	1.3 (0.05)	41.0	4.9
11	CRCP	980.1 (62.1)	23.4	1.0 (0.04)	44.4	10.6
12	Comp.	634.5 (40.2)	20.6	4.1 (0.16)	35.5	9.8
13	JPCP	1521.5 (96.4)	22.4	1.3 (0.05)	45.5	26.2
14	Flexible	1257.9 (79.7)	26.8	7.9 (0.31)	40.3	4.6
15	Flexible	847.5 (53.7)	14.4	5.3 (0.21)	36.0	11.3
16	Flexible	637.6 (40.4)	23.6	0.8 (0.03)	35.6	6.2
17	Flexible	1336.8 (84.7)	30.6	3.6 (0.14)	44.9	3.6
18	Flexible	1149.0 (72.8)	25.8	2.5 (0.10)	32.4	10.6

SUMMARY OF FINDINGS

A summary of the condition of all flexible, composite, and rigid pavements as well as test results are presented in Table 14 through Table 16.

Table 14. Summary data for flexible pavements

Site	01	03_{S1-3}	03_{S2}	06	14	15	16	17	18
Age	34	34		25	6	37	39	42	5
Surface Age	11	9		7	6	17	13	11	3
AADT (x1000)	20	12		25	8.5	20	20	27	22
Trucks	1100	1320		750	765	6800	4280	5130	5940
Deflections (mils)									
D_1	6.1	3.9	7.4	7.3	3.6	7.9	3.7	5.9	3.5
COV (%)	25	22	17	15	20	10	16	16	18
D_7	2.2	1.2	2.7	1.1	0.6	1.5	0.9	1.4	0.9
COV (%)	27	46	28	22	36	17	32	21	32
D_9	1.3	0.7	1.7	0.7	0.4	0.8	0.5	0.9	0.6
COV (%)	30	51	33	21	42	20	35	25	37
Thickness (in)									
HMA	9.4	12	12	10.7	8.4	11.8	11.5	13.3	14.5
Asphalt OGDL	-	-	-	-	2.7	-	-	-	3
Aggr. Base	-	-	8	5.8	-	15	18	-	21
CTA	5.9	8	-	-	8	-	-	-	-
Cement Stab. Subg.	-	-	-	6	-	-	-	-	-
Subgrade	sandy silt	fine red silt, brown sandy silt, some weathered rock		dry sandy silt to red silty clay	N/A	red brown silty clay w/gravel, fill material	fill w/comp. clay & gravel, damp clay w/silt	crushed stone	sandy silty clay
Laboratory Characterization (ksi)									
SM @ 25°C	746	893		541	637	920	610	643	600
BM @ 25°C	433	704		428	594	484	993	656	721
Back. Moduli (ksi)									
HMA	462	540	557	231	522	266	582	403	567
COV (%)	31	34	32	16	22	16	15	18	19
Asphalt OGDL					205				175
COV (%)					25				23
Aggr. Base			62	40		40	99		92
COV (%)			31	28		23	22		22
CTA	1256	429			411				
COV (%)	42	40			26				
Cement Stabilized Subgrade				382					
COV				30					
Subgrade	16	36	14	40	68	21	36	30	46
COV (%)	35	44	42	25	29	20	29	22	32
Condition									
Roughness (in/mi)	96.9	76.2		63.7	79.7	53.7	40.4	84.7	72.8
CCI	75	69		81	100	90	92	92	100
LDR	96.7	95.8		96.3	99.9	89.7	99.8	94.2	100
NDR	74.5	68.6		80.5	99.9	92.3	91.6	92	100
Rutting (in)	0.12	0.11		0.13	0.31	0.21	0.03	0.14	0.10
Friction (SN40)	37.9	39.9		44.4	40.3	36.0	35.6	44.9	32.4

Table 15. Summary data for composite pavements

Site	02	05	08	09	10	12
Age	34	32	72	23	24	14
Surface Age	12	13	1	6	9	6
AADT (x1000)	15	21	58	24.5	37	19.5
Trucks	1680	880	1740	1000	3300	5070
Deflections (mils)						
D_1	3.8	4.2	10.9	3.8	2.6	2.3
COV (%)	14	18	34	25	14	13
D_7	1.7	1.8	4.8	1.5	1.1	0.7
COV (%)	21	31	37	23	13	14
D_9	1.2	1.2	3.3	1.0	0.8	0.5
COV (%)	24	33	38	22	12	17
Thickness (in)						
HMA	4.25	4.25	7.8	3.75	3.9	14.7
Asphalt OGDL	-	-	-	-	-	2.8
CRCP	8	8		8.5	8	-
JPCP	-	-	7.6	-	-	9
Agg. Base	-	6	-	-	-	-
CTA	-	-	-	6	6	-
Subgrade	reddish-brown sandy silt w/mica	dry silt/fine sand	brown fine silty sand	yellow silt clay and silty clay w/mica	silty clay w/fine gravel	cement stabilized subgrade
Laboratory Characterization						
SM @ 25°C (ksi)	651	779	351	975	436	755
BM @ 25°C (ksi)	530	635	N/A	N/A	601	963
CRCP (psi)	5930	6990	9020	8310	5240	-
JPCP (psi)	-	-	-	-		N/A
Back. Moduli (ksi)						
HMA	339	369	212	267	574	594
COV (%)	21	13	37	51	5	19
Asphalt OGDL						113
COV (%)						34
CRCP	4610	3892	1489	2299	2588	
COV (%)	26	25	49	39	42	
JPCP						3626
COV (%)						29
Agg. Base		68				
COV (%)		28				
CTA				331	540	
COV (%)				43	25	
Subgrade	38	35	13	43	53	85
COV (%)	23	29	20	22	15	15
Condition						
Roughness (in/mi)	87.1	75.3	72.2	82.8	66.0	40.2
CCI	87	77	97	83	98	96
LDR	86.7	77.3	100	99.7	100	95.8
NDR	87.5	88.1	97.3	83.1	97.8	97.2
Rutting (in)	0.22	0.26	0.00	0.05	0.05	0.16
Friction (SN40)	32.7	45.9	45.2	37.0	41.0	35.5

Table 16. Summary data for rigid pavements

Site	04	11	07	13
Age	17	12	7	8
Surface Age	17	12	7	8
AADT (x1000)	12	11	56	60
Trucks	1320	2750	1680	4200
Deflections (mils)				
D_1	4.9	2.0	2.2	1.5
COV (%)	18	17	56	13
D_7	2.4	1.1	0.8	1.2
COV (%)	24	22	21	15
D_9	1.5	0.8	0.7	0.7
COV (%)	25	21	15	15
Thickness (in)				
CRCP	8	9.5	-	-
JPCP	-	-	11.5	11
Asphalt OGDL	-	-	3	3
Cement OGDL	-	4	-	-
Cement Stab. Aggr.	4	6	6	6
Cement stab. borrow	-	-	-	6
Cement stab. Subgr.	6	-	-	-
Subgrade	reddish-brown sandy silt & decomposed rock	crushed stone & reddish-brown sandy clay	very wet gray crushed run material & red brown wet silt	N/A
Laboratory Characterization (psi)				
CRCP	7470	7060	-	-
JPCP	-	-	7660	8240
Back. Moduli (ksi)				
CRCP	4032	4323		
COV (%)	14%	23%		
JPCP			3264	6211
COV (%)			76%	15%
Asphalt OGDL			145	94
COV (%)			59%	60%
Cement OGDL		213		
COV (%)		25%		
Cement Stab. Aggr.	100	709	596	476
COV (%)	37%	15%	65%	31%
Cement stab. Borrow				123
COV (%)				52%
Cement stab. Subgr.	47			
COV (%)	31%			
Subgrade	19	53	68	56
COV (%)	25%	26%	18%	21%
Condition				
Roughness (in/mi)	97.4	62.1	56.3	96.4
CCI	99	98	100	98
CDR	99.8	98.9	-	-
CPR	98.7	98.3	-	-
SDR	-	-	99.8	97.1
Rutting (in)	0.09	0.04	0.02	0.05
Friction (SN40)	37.5	44.4	35.1	45.5

The following findings were obtained:

- As expected, all the sites are performing satisfactorily and show very low structural distresses. This was expected because the research team aimed at selecting the "best performing" pavement sections in the Commonwealth for this investigation.

- Observation of the cores showed indication of HMA deterioration, probably stripping, in some for the sections. This deterioration is very noticeable in several of the cores in Sites 03 and 06.

- The GPR can determine the total thickness of the surface layers (HMA or PCC) with a high degree of accuracy, especially if calibrated with a minimum number of cores. The average absolute thickness error varied between 1.8% for Site 04 to 8.4% for Site 16, with an overall average of approximately 4.7%. The concrete thickness may not be determined from the GPR data in the case of composite pavements if its bottom interface produces a very low reflection that is not detected by the GPR receiver.

- Although the backcalculation software produced reasonable results for most of the sites, some difficulties were experienced. In particular the modulus of the HMA was underestimated for some of the flexible and composite pavements. Examples include Sites 06 and 15 for the flexible pavements and Sites 08 and 09 for the composite pavements. In addition, the PCC modulus in Site 13 is too high. It appears to be a "compensating" problem. The 21-A and OGDL moduli are low, while PCC modulus is high.

- Most of the fatigue cracks observed are longitudinal cracks in the wheelpath, probably top-down cracks. Taking cores on the cracks should help determine the nature of these cracks.

- The historical records available in VDOT databases are not complete, several differences were observed between the pavement layers and thicknesses obtained from documents and those actually measured of the field cores and by the GPR.

- Sites 09 and 10 have similar designs but Site 10 seems to be performing better although it has higher truck traffic. This could be due to a better performance of the surface mix in section 10, as suggested by the relatively lower HMA resilient modulus at Site 09. While section 09 was resurfaced with a standard SuperPave mix, section 10 used an SMA. The different performance could also be attributed to the presence of the mica in the Site 09 subgrade. Mica is sensitive to moisture and hence reduces the resilient modulus of the subgrade and increases the surface deflection as shown in the FWD results. Over time, such an effect becomes more pronounced. In this case, it was clear that the material characteristics of the pavement system have more effect on the performance than the traffic loading.

- Comparison of the various sites seems to indicate that there is more rutting in composite pavements (Sites 02, 05, and 12).

CONCLUSION

The results of the field investigation suggest that "premium" pavement designs to provide adequate service for at least 40 years can be obtained. To achieve that, appropriate material design and construction are particularly important to withstand the traffic and environmental loading. However, the selection of the most appropriate pavement type and design should be controlled by the site, material availability, and economics (life-cycle cost analysis) among others.

RECOMMENDATIONS

Based on the results of this first phase of the project, these follow-up investigations are recommended:

- To complement the data collected from the best performing sites, a field evaluation of sites thought to have average and poor performance need to be conducted. This will allow the conducting of a rugged life-cycle cost analysis to optimize the premium pavement design selection including rehabilitation strategies.

- Characterize the pavement materials, collected from the sites, in accordance with the proposed testing procedures suggested by the National Cooperative Highway Research Project (NCHRP) 1-37 on Mechanistic Empirical (M-E) pavement design.

- Utilize the collected data from the sites, to develop a premium pavement design and test using an Accelerated Pavement Testing (APT) facility for major distresses (e.g. rutting, fatigue, and top-down cracking for flexible pavement)

- Continue periodic monitoring of these sites; especially at the time of rehabilitation. In addition, the analysis could also be enhanced by obtaining the condition of the various sites at time of rehabilitation, if available. Better traffic data (e.g., load spectra) would also be useful when comparing the performance of the various pavement designs.

In addition, the extensive filed investigations allowed recommending some improvements to the pavement evaluation procedures*:*

- It may be necessary to assess the accuracy of the historical pavement management records. Several discrepancies were observed for the sites investigated.

- It may be useful to continue the development of VDOT's backcalculation package by incorporating an interactive backcalculation procedure.

- VDOT should consider the use of FWD and GPR for quality control and assurance.

ACKNOWLEDGMENTS

The authors acknowledge the contribution to the successful completion of the project of the following individuals: L. E. (Buddy) Wood, Jr., David Mokarem, Brian Diefenderfer, and Troy Deeds from VTRC; Kun Jiang, Carlos Gramajo, Edgar de Leon, and Mostafa Elseifi from VTTI; participating VDOT district materials, geotechnical, and traffic control crews; and the project steering panel.

REFERENCES

American Society for Testing and Materials, ASTM D1586, Standard Test Method for Penetration Test and Split-Barrel Sampling of Soils, *Annual Book of ASTM Standards*, Soil and Rock, Vol. 04.08, Philadelphia, PA, 2000.

American Society for Testing and Materials, ASTM D2488, Standard Practice for Description and Identification of Soils (Visual-Manual Procedure), *Annual Book of ASTM Standards*, Soil and Rock, Vol. 04.08, Philadelphia, PA, 2000.

American Society for Testing and Materials, ASTM D4123, Standard Test Method for Indirect Tension Test for Resilient Modulus of Bituminous Mixtures, *Annual Book of ASTM Standards*, Road and Paving Materials, Vol. 04.03, Philadelphia, PA, 1995.

American Society for Testing and Materials, ASTM C39/C39M-99, Standard Test Method for Compressive Strength of Cylindrical Concrete Specimens, *Annual Book of ASTM Standards*, Concrete and Aggregate, Vol. 04.02, Philadelphia, PA, 1999.

American Society for Testing and Materials, ASTM E 1926, Practice for Computing International Roughness Index from Longitudinal Profile Measurements, *Annual Book of ASTM Standards*, Road and Paving Materials, Vol. 04.03, Philadelphia, PA, 1998.

American Society of Testing and Materials, ASTM E524, Specification for Standard Smooth Tire for Pavement Skid-Resistance Tests, *Annual Book of ASTM Standards*, Road and Paving Materials, Vol. 4.03, Philadelphia, PA, 2000.

American Society of Testing and Materials. ASTM E274, Standard Test Method for Skid Resistance of Paved Surfaces Using a Full-Scale Tire, *Annual Book of ASTM Standards*, Road and Paving Materials, Vol. 4.03, Philadelphia, PA, 2000

Kim, R. Y., Daniel, J. S., and Wen, H., *Fatigue Performance Evaluation of Westrack Asphalt Mixtures Using Viscoelastic Continuum Damage Approach*, Final Report, No. FHWA/NC/2002-004, North Carolina Department of Transportation, Raleigh, NC, 2002.

Virginia Department of Transportation, *A Guide To Evaluating Pavement Distress Through The Use Of Video Images*, Maintenance Division, Richmond, 2001.

Virginia Department of Transportation, *Development and Implementation of Pavement Condition Indices for the Virginia Department of Transportation* (Phase I and II, Flexible and Rigid Pavements), Maintenance Division, Richmond, VA, 2002.